(*S*)-Mandelate Dehydrogenase from *Pseudomonas putida*: Mechanistic Studies with Alternate Substrates and pH and Kinetic Isotope Effects†

Isabelle E. Lehoux and Bharati Mitra*

Department of Biochemistry and Molecular Biology, School of Medicine, Wayne State University, Detroit, Michigan 48201

Received January 5, 1999; Revised Manuscript Received February 19, 1999

ABSTRACT: (*S*)-Mandelate dehydrogenase from *Pseudomonas putida*, a member of the flavin mononucleotide-dependent α-hydroxy acid oxidase/dehydrogenase family, oxidizes (*S*)-mandelate to benzoylformate. The enzyme was purified with a carboxy-terminal histidine tag. Steady-state kinetic parameters indicate that it preferentially binds large substrates. A good correlation was obtained between the k_{cat}, the substrate kinetic isotope effect (KIE), and the pK_a of the substrate α-proton. The k_{cat} decreased and the KIE increased for substrates whose α-protons have pK_as higher than that of mandelate. These results support a mechanism involving a carbanion intermediate but are difficult to reconcile with one involving a direct hydride transfer. pH effects on steady-state parameters were determined with (*S*)-mandelate and a slow substrate, (*R*,*S*)-3-phenyllactate. The k_{cat}/K_m pH profile shows that two groups with apparent pK_as of 5.5 and 8.9 in the free enzyme are important for activity. These pK_as are shifted to 5.1 and 9.6 on binding (*S*)-mandelate, as shown in the k_{cat} pH profile. The pH dependence of the KIEs suggests that the residues with these pK_as are involved in the α-carbon−hydrogen bond-breaking step. pH dependencies of the inhibition constants for competitive inhibitors identified these residues as histidine 274 and arginine 277. We propose that histidine 274 is the base that abstracts the substrate α-proton and arginine 277 is important for substrate binding as well as stabilization of the carbanion/enolate intermediate.

(*S*)-Mandelate dehydrogenase (MDH),[1] an enzyme in the mandelate metabolic pathway in *Pseudomonas putida* (ATCC 12633), catalyzes the oxidation of (*S*)-mandelate to benzoylformate:

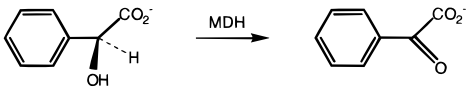

MDH is a member of a family of FMN-dependent α-hydroxy acid dehydrogenases/oxidases that includes glycolate oxidases from mammals and plants, lactate monooxygenase from *Mycobacterium smegmatis*, lactate oxidase from *Aerococcus viridans*, flavocytochrome b_2s (lactate and mandelate dehydrogenases) from yeast, and long-chain α-hydroxy acid oxidase from rat kidney (*1*, *2*). Though all the enzymes of this family specifically oxidize the (*S*)-enantiomer of an α-hydroxy acid to an α-keto acid, the ultimate oxidant depends on the particular enzyme. Oxygen is the electron acceptor for the oxidases, whereas the flavocytochrome b_2s utilize an intramolecular heme. The membrane-associated bacterial dehydrogenases, including MDH, transfer the electron pair from the reduced FMN to a component of the electron transport chain in the membrane.

Given the high sequence homology in this enzyme family as well as similarities between the three-dimensional structures of glycolate oxidase from spinach and flavocytochrome b_2 from *Saccharomyces cerevisiae*, it is apparent that the mechanism of the first half-reaction (substrate oxidation and FMN reduction) is similar for the entire family. Additionally, the oxidation of α-amino acids by the FAD-dependent D-amino acid oxidase family may be mechanistically similar to that of α-hydroxy acids. A number of enzymes in the α-hydroxy acid oxidase/dehydrogenase family have been extensively studied, most notably lactate monooxygenase from *M. smegmatis* (*3*) and flavocytochrome b_2 from *S. cerevisiae* (*4*). Some of the mechanistic questions have revolved around the issue of where the electron pair resides when the substrate α-carbon−hydrogen bond is broken. The majority of the experimental data suggest that the reaction proceeds through the formation of a carbanion intermediate generated by the loss of the α-proton. However, a mechanism involving the direct transfer of a hydride equivalent to FMN has not been unequivocally ruled out. Recent mechanistic studies with D-amino acid oxidase and lactate oxidase have questioned the validity of a "carbanion intermediate" mechanism (*5*, *6*). Structural analysis of D-amino acid oxidase has led Mattevi and co-workers (*7*) to propose a direct hydride transfer mechanism.

We have begun mechanistic and structural studies of MDH, an enzyme that belongs to the α-hydroxy acid oxidase/dehydrogenase family but has some notable differences. MDH is the only enzyme whose physiological substrate is an α-hydroxy acid with β-unsaturation; the pK_a of its α-proton is expected to be smaller than those of saturated

† This work was supported by NIH Grant GM-54102 and by a Wayne State University research grant.

* Address correspondence to this author: e-mail bmitra@med.wayne.edu.

[1] Abbreviations: DCPIP, dichloroindophenol, sodium salt; FAD, flavin adenine dinucleotide; FMN, flavin mononucleotide; IPTG, isopropyl β-thiogalactopyranoside; KIE, kinetic isotope effect; LB medium, Luria−Bertani medium; MDH, (*S*)-mandelate dehydrogenase; PCR, polymerase chain reaction; PMS, phenazine methosulfate; SDS−PAGE, sodium dodecyl sulfate−polyacrylamide gel electrophoresis.

10.1021/bi990024m CCC: $18.00
Published on Web 04/13/1999

substrates. Additionally, mandelate is rather bulky and sterically constrained compared to the small, aliphatic substrates utilized by the other members of this family. MDH is also a member of an emerging subgroup in this enzyme family, comprising of membrane-bound bacterial enzymes that are part of metabolic pathways and do not use oxygen at an appreciable rate.

In this work, we have purified MDH as a histidyl-tagged protein and characterized it as a representative member of the α-hydroxy acid oxidase/dehydrogenase family. We also present steady-state kinetic parameters for aliphatic and aromatic substrates with highly different pK_as of the α-proton. Our results show that when substrates without any β unsaturation are utilized, the turnover rate decreases by 2−4 orders of magnitude; the substrate kinetic isotope effect increases concomitantly, implying that carbon−hydrogen bond cleavage becomes more rate-limiting. These results are consistent with a "carbanion intermediate" mechanism but are difficult to reconcile with a "hydride transfer" mechanism. Data obtained from α-hydroxy acids with different sizes of side chains suggest that the active site of MDH has a large, hydrophobic substrate-binding pocket that confers specificity toward large substrates. We also present detailed pH studies of the steady-state kinetic parameters, including substrate kinetic isotope effect, for (*S*)-mandelate as well as (*R,S*)-3-phenyllactate, a very slow substrate—the first report of its kind for the α-hydroxy acid-utilizing enzymes. Our results show that a residue with an apparent pK_a of 5.5 in the free enzyme has to be deprotonated for activity. A second residue with an apparent pK_a of 8.9 in the free enzyme has to be protonated for activity as well as substrate binding: its mechanistic role appears to be stabilization of the carbanion intermediate. Studies with competitive inhibitors coupled with structural information available for two of the homologous enzymes indicate that the apparent pK_as of 5.5 and 8.9 belong to histidine 274 and arginine 277, respectively.

EXPERIMENTAL PROCEDURES

Materials

Oligonucleotides were purchased from Integrated DNA Technologies, Coralville, IA. Ni^{2+} resin was from Invitrogen or Qiagen. 2-Hydroxyisovaleric acid, 2-hydroxycaproic acid, 2-hydroxyoctanoic acid, 3-phenyllactic acid, and 2-hydroxybutyric acid, sodium salt, were from Fluka; 3-indolelactic acid, 2-hydroxyvaleric acid, 2-hydroxyisocaproic acid and (*S*)- and (*R,S*)-mandelic acids were from Aldrich. 2-Hydroxy-3-butynoic acid was from TCI. Indole-3-glyoxylyl chloride was from Lancaster. Vinylglycolic acid and the sodium salt of indole-3-glycolic acid were synthesized as described below. Deuterium oxide and sodium borodeuteride were from Cambridge Isotope Laboratories. All other chemicals were of the highest commercial grade and were obtained from Aldrich and Sigma.

[α-^{2}H]-(*R,S*)- and (*S*)-mandelic acids were prepared from the protio compounds by use of wild-type mandelate racemase and the H297N mutant of mandelate racemase respectively, to catalyze the exchange of the α-proton with solvent deuterium (the mandelate racemase enzymes were a gift from Dr. John A. Gerlt). Proton NMR confirmed that deuteration was >99%.

Chemical Syntheses

[α-^{1}H]- and [α-^{2}H]-(R,S)-Vinylglycolic Acids. (*R,S*)-Vinylglycolic acid was synthesized as described (*8*). [α-^{2}H]-(*R,S*)-Vinylglycolic acid was prepared from the protio compound by use of wild-type mandelate racemase (*8*); it was 90% deuterated. The extent of deuteration was taken into account when substrate kinetic isotope effects were measured.

[α-^{1}H]- and [α-^{2}H]-(R,S)-2-Hydroxyoctanoic and [α-^{1}H]- and [α-^{2}H]-(R,S)-3-Phenyllactic Acids. The [α-^{1}H]- and [α-^{2}H]-2-hydroxy acids were prepared by reducing the corresponding α-keto acids. Specifically, to a solution of the 2-oxo acid in water, ∼1.1 equiv of solid $NaBH_4$ (or $NaBD_4$) were added slowly. The mixture was stirred for 90 min at room temperature and quenched by slowly adding 6 N HCl until the pH was <3. The acidic solution was left stirring for 2−3 h. The acid was then extracted 3−5 times with ether, the organic phase was rotary-evaporated, and the product was dried further by lyophilization overnight. Yields were 50−70%. NMR revealed no impurities in any of the four compounds. 2-Hydroxyoctanoic and 3-phenyllactic acids were >99% deuterated as evidenced by NMR.

[α-^{1}H]- and [α-^{2}H]-(R,S)-Indole-3-glycolic Acids, Sodium Salts. The methyl ester of indole-3-glyoxylic acid was prepared as follows. Five grams (0.024 mol) of indole-3-glyoxylyl chloride (Lancaster) were mixed slowly with 3.62 mL (0.026 mol) of triethylamine in 50 mL of methanol and incubated for several hours at room temperature. The solid was isolated by filtration, washed with methanol, and resuspended in ethyl acetate. The organic phase was washed with 10% sodium bicarbonate solution in water and dried over anhydrous sodium sulfate. The solvent was eliminated by rotary evaporation and then by lyophilization overnight. The pale yellow ester was obtained in 3.5 g yield (70%), melting point 232 °C. ^{1}H NMR (C_2D_6O) revealed the following resonances: δ (ppm) O−C**H$_3$** 3.9 (s, 3 H); aromatic **H** 7.3 (m, 2 H), 7.6 (m, 1 H), 8.3 (q, 1 H) and 8.5 (d, 1 H); N**H** 11.6 (s, 1 H).

The 2-oxo ester was reduced to the 2-hydroxy ester with $NaBH_4$ (or $NaBD_4$ when the deuterated substrate was prepared). The ester (1.5 g, 7.4 mmol) was stirred in 100 mL of methanol under N_2. $NaBH_4$ (or $NaBD_4$) was added slowly till the reduction was complete as monitored by TLC. The reduced hydroxy ester could be separated from the starting keto ester on TLC with the solvent system CH_2Cl_2/CH_3OH 39:1. A clear, slightly yellow solution was obtained. The solvent was evaporated and the semisolid product was dissolved in ethyl acetate. The organic phase was washed twice with 10% aqueous sodium bicarbonate solution, dried over Na_2SO_4, and filtered, and the solvent was evaporated. At this stage, TLC revealed that the 2-hydroxy ester product contained minor impurities. Reduction was confirmed by ^{13}C NMR and ^{1}H NMR (C_2D_6O), δ (ppm) OC**H$_3$** 3.7 (s, 3 H); Cα-**H** 4.5 (d, 1 H); O**H** 5.5 (d, 1 H); aromatic **H** 7.0−7.14 (m, 2 H), 7.3−7.4 (m, 2H), and 7.7 (d, 1 H); N**H** 10.2 (s, 1 H).

To prepare the sodium salt of (*R,S*)-indole-3-glycolic acid from the ester, the product from the above step was

resuspended in a minimum amount of ether. Water was added in large excess (40:1 v/v) followed by 1 M NaOH. Saponification was monitored by TLC (the acid migrated on TLC in 40% methanol in dichloromethane) and by measuring the pH of the aqueous phase. After several hours when the pH of the aqueous phase was ~7.0, the remaining ether was rotary-evaporated and the aqueous phase was washed twice with ethyl acetate to eliminate the impurities of the previous step. The aqueous phase containing the sodium salt of the acid was lyophilized. The final yield was 10−20% of the starting indole-3-glyoxylyl chloride. The product was slightly pink in color. ^{1}H NMR (D_2O), δ (ppm) Cα-**H** 5.1 (s, 1 H); aromatic **H** 6.9 (t, 1 H), 7.0 (t, 1 H), 7.2 (s, 1 H), 7.3 (d, 1 H), and 7.5 (d, 1 H).

Methods

Genetic Engineering Methods: Hexahistidyl-Tagged MDH. The expression vector for MDH in *Escherichia coli*, pBM (*9*), was modified by engineering a hexahistidyl tag at the carboxyl terminus of MDH by PCR methods. The histidine tag was placed immediately preceding the termination codon, by use of the oligonucleotide 5′-GCG-CTGCAG-TCA-ATGGTGATGGTGATGGTG-TGC-GTG-TGT-3′. PCR experiments were carried out with Vent DNA polymerase (New England Biolabs). The histidine-tagged MDH was expressed by growing transformed cells in LB medium supplemented with 100 μg/mL ampicillin till the absorbance at 590 nm was 1.0, followed by overnight induction with 0.5 mM IPTG.

Enzyme Purification. The carboxy-terminal histidyl-tagged MDH was purified as described (*9*) with the following modification. Following solubilization of the protein from the membrane suspension with the detergent Triton X-100, it was loaded on a 5 × 1.25 cm Ni-resin column equilibrated with buffer A (20 mM potassium phosphate, pH 7.5, 10% ethylene glycol, and 0.05% Triton X-100 or 0.5−1% Tween 80). The column was washed extensively first with buffer A and second with buffer A containing 50 mM imidazole. Finally, the pure protein was eluted with 300 mM imidazole in buffer A. MDH was immediately passed through a Sephadex G-25 column equilibrated in buffer A to remove imidazole and concentrated. Finally, the buffer was made up to 20% ethylene glycol and the protein was stored in aliquots at −70 °C.

Determination of Protein Concentration. Protein concentrations were usually measured by estimating the flavin content. Specifically, the protein solution was boiled for 5 min at 100 °C and the precipitated protein was centrifuged for 5 min at 15000*g*. The amount of flavin released was determined by measuring the absorbance of the supernatant at 445 nm, using an extinction coefficient of 12 500 M^{-1} cm^{-1} at pH 7.5 for free FMN. The protein concentration was then estimated by assuming a 1:1 molar ratio for FMN and MDH subunit. Protein concentrations were also determined with the bicinchoninic acid reagent (Sigma), with bovine serum albumin as standard.

Determination of the Extinction Coefficient of MDH-Bound FMN. The extinction coefficient of MDH at 460 nm and in 20 mM potassium phosphate, pH 7.5, containing 1% Tween 80 and 20% ethylene glycol, was determined by comparing the absorbance of the enzyme-bound flavin with that of free flavin released on boiling the enzyme for 5 min at 100 °C. The absorbance of enzyme-bound FMN was corrected for light scattering by the detergent present in the buffer.

Determination of the pK_a of Enzyme-Bound FMN. The enzyme was equilibrated in 20 mM phosphate buffer containing 1% Tween 80 and 10% ethylene glycol at 4 °C. The pH was raised by small additions of concentrated potassium hydroxide solutions directly in a cuvette; in each case, the dilution was less than 0.03%. Following each addition, the absorbance and pH were measured simultaneously. The data were fit to a modified version of the Henderson−Hasselbalch equation where A_{obs} = absorbance at a particular wavelength at any pH and A and B are the limiting absorbance values at the same wavelength at low and high pH, respectively:

$$A_{obs} = \frac{A + B10^{pH-pK_a}}{1 + 10^{pH-pK_a}} \quad (1)$$

Formation of a Reversible Sulfite Adduct of Enzyme-Bound Flavin. MDH forms a reversible adduct of FMN with sulfite. To determine the dissociation constant of the FMN−sulfite adduct, 11 μM MDH was incubated with different concentrations of sodium sulfite at 4 °C, in 20 mM phosphate buffer, pH 7.5, containing 0.05% Triton X-100 and 5% ethylene glycol, and the absorbance change at 460 nm was measured. The experiment was also repeated in a buffer containing 100 mM phosphate, pH 7.5, with 0.05% Triton X-100. The data were fit to eq 2, where the concentration of the adduct, $MDH{\cdot}SO_3^{-2}$, is proportional to the change in the absorbance at 460 nm of the fully oxidized MDH upon addition of sulfite:

$$K_d = \frac{[MDH_{(free)}][SO_3^{2-}{}_{(free)}]}{[MDH{\cdot}SO_3^{2-}]} \quad (2)$$

Enzyme Assays. Activity assays were routinely performed at 20 °C, in 0.1 M phosphate buffer, pH 7.5, by measuring the reduction of 50−100 μM DCPIP at 600 nm in the presence of 1.0 mg/mL BSA and 1 mM phenazine methosulfate (9). When DCPIP was used as an electron acceptor, the maximal activity with (*S*)-mandelate is obtained when BSA and PMS are included in the assay. Potassium ferricyanide was also tested as an electron acceptor by following its reduction at 420 nm; in this case, phenazine methosulfate and BSA were omitted from the assay buffer. Extinction coefficients used for DCPIP were 21.6 mM^{-1} cm^{-1} at 600 nm and pH 7.5 and 8.6 mM^{-1} cm^{-1} at 522 nm in the pH range 4−9.5, and for ferricyanide, 1.1 mM^{-1} cm^{-1} at 420 nm.

Isotope Effects. Isotope effects were obtained in the standard assay buffer at pH 7.5 with the exception of the pH studies. For solvent isotope effects, 0.1 mM potassium phosphate was made up in D_2O. BSA (1 mg/mL) and 100 μM DCPIP were added. The solution was lyophilized and the solids were redissolved in D_2O. The solvent isotope effects were measured at pD 7.5, which was calculated as pH + 0.4 (*10*).

Irreversible Inactivation by 2-Hydroxy-3-butynoic Acid. To determine the kinetics of inactivation, 3 μM MDH was incubated with different concentrations of 2-hydroxy-3-butynoate and 150 μM DCPIP, in a total volume of 150 μL

at 25 °C. The inhibitor concentrations ranged from 10 to 40 mM. The buffer used was 20 mM phosphate, pH 7.5, containing 0.1% Triton X-100 and 10% ethylene glycol. At known time intervals (0−17 min), 10 μL aliquots were removed from the incubation mixture and diluted into 1.0 mL of standard assay buffer. The assays were initiated by the addition of (*S*)-mandelate. The half-time of inactivation at each concentration of 2-hydroxy-3-butynoate, $t_{1/2}$, was obtained by a semilog plot of remaining activity versus time. The inhibition constant K_i and the rate of inactivation, k_i, were calculated from eq 3, where [I] is the concentration of inhibitor:

$$\frac{t_{1/2}}{0.693} = \frac{1}{k_i} + \frac{K_i}{k_i[I]} \tag{3}$$

The turnover-to-inactivation ratio of 2-hydroxy-3-butynoate for MDH was calculated from the ratio of k_{cat} to k_i. This ratio was also determined by a more direct method. MDH (0.03 μM) was incubated with 80 mM 2-hydroxy-3-butynoate and 150 μM of DCPIP in a total volume of 0.5 mL. The decrease in absorbance at 522 nm due to the reduction of DCPIP was monitored until there was no more change due to the inactivation of MDH. The turnover-to-inactivation ratio was directly calculated from the amount of DCPIP reduced during the experiment.

pH Dependence of Kinetic Parameters. The buffer used over the pH range 4.5−9.5 (universal buffer) was made up of 0.025 M boric acid, 0.025 M potassium phosphate, 0.025 M Tris, and 0.025 M succinic acid. At each pH, the final ionic strength was maintained at 0.18 with the addition of KCl. Assays were performed by measuring the decrease in absorbance of DCPIP at 522 nm in the presence of 1 mg/mL BSA and 1 mM PMS. The DCPIP concentration was kept between 0.22 and 0.24 mM, which is >10-fold the K_m for DCPIP determined under these conditions. When 3-phenyllactate was the substrate, PMS did not affect the rates and was excluded from the assay buffer. However, for this substrate, micromolar quantities of enzyme had to be used due to the very low activity with this substrate. Therefore, to avoid aggregation of the enzyme, especially at low pHs over the time scale of the assays, 0.2% Triton X-100 was included in the assay. The extinction coefficient of DCPIP was remeasured at 522 nm in the presence of 0.2% Triton X-100 and 1 mg/mL BSA at each pH. V_{max} and K_m for [α-^{1}H]- and [α-^{2}H]-(*S*)-mandelate or (*R,S*)-3-phenyllactate were obtained from eq 4.

The inhibition constants for the competitive inhibitors were determined with the same universal buffer system and identical assay conditions. Inhibitor concentrations were varied as follows: 0−40 mM for 2-phenylacetate, 0−110 mM for (*S*)-1-phenyl-1,2-ethanediol, 0−30 mM for (*S*)-2-methoxy-2-phenylacetate, and 0−20 mM for (*S*)-3-phenyllactate. (*S*)-Mandelate concentrations were held constant at 1 or 2-fold K_m. The data were fitted to eq 5.

The pH dependence of the kinetic parameters for (*S*)-mandelate was also determined by a different protocol and a different buffer system. Sodium acetate (0.1 M) was used for pH 4.5−5.5. Between pH 5.5 and 9.5, a buffer made up of 0.1 M Mes, 0.052 M Tris, and 0.052 M ethanolamine was used; this buffer maintains a constant ionic strength of 0.1 over this pH range (*11*). In this protocol, BSA and PMS were omitted from the assays. Initial velocities were obtained as a function of pH by varying (*S*)-mandelate concentrations at different fixed nonsaturating concentrations of DCPIP, the second substrate in our assays. Data were fitted to the double-reciprocal form of eq 4 to generate slopes and intercepts for each line. The *V*/*K* parameter for (*S*)-mandelate was generated from the parallel line patterns that were obtained. The V_{max} and the *V*/*K* for DCPIP were obtained as the intercept and slope of the intercept replot.

pH Data Analysis. Substrate saturation kinetic data were fitted to eq 4. Inhibition constants for the competitive inhibitors were calculated from eq 5, where [I] is the concentration of the inhibitor:

$$v = \frac{V_{max}[S]}{K_m + [S]} \tag{4}$$

$$v = \frac{V_{max}[S]}{K_m(1 + [I]/K_i) + [S]} \tag{5}$$

The pH dependence of k_{cat} as well as k_{cat}/K_m for (*S*)-mandelate was fitted to a bell-shaped curve described by eq 6, where *Y* is the limiting value at intermediate pH:

$$y = \frac{Y}{1 + 10^{pK_1 - pH} + 10^{pH - pK_2}} \tag{6}$$

The pH dependence of k_{cat} for (*R,S*)-3-phenyllactate was fitted to eq 7, where Y_I and Y_H are the limiting plateau values at intermediate and high pHs, respectively:

$$y = \frac{Y_I + Y_H 10^{pH - pK_2}}{1 + 10^{pK_1 - pH} + 10^{pH - pK_2}} \tag{7}$$

The pH dependence of the K_is for the competitive inhibitors 2-phenylacetate, (*S*)-3-phenyllactate, and (*S*)-2-methoxy-2-phenylacetate were fitted to eq 8, and the K_i for (*S*)-1-phenyl-1,2-ethanediol was fitted to eq 9. Equation 8 describes a fit where the K_i increases from a lower limiting value, Y_L, at acidic pH to an intermediate limit, Y_I, at neutral pH and finally increases rapidly at alkaline pH:

$$y = \frac{(Y_L + Y_I 10^{pH - pK_2})(1 + 10^{pH - pK_2})}{(1 + 10^{pH - pK_1})} \tag{8}$$

$$y = Y_L(1 + 10^{pK - pH}) \tag{9}$$

Instrumentation and Data Analysis. UV−visible spectra were recorded with a Cary 1E Varian spectrophotometer. Data were analyzed with KaleidaGraph for the Macintosh (Synergy Software).

RESULTS

Purification and Spectral Properties of MDH. We previously reported the expression of the gene for (*S*)-mandelate dehydrogenase from *P. putida* in *E. coli* and its purification by anion-exchange chromatography following solubilization with detergents from the cytoplasmic membranes (*9*). However, we observed that even though the protein appeared pure on SDS−PAGE, there was an impurity associated with it that had a UV−vis absorption peak at 414 nm, in addition

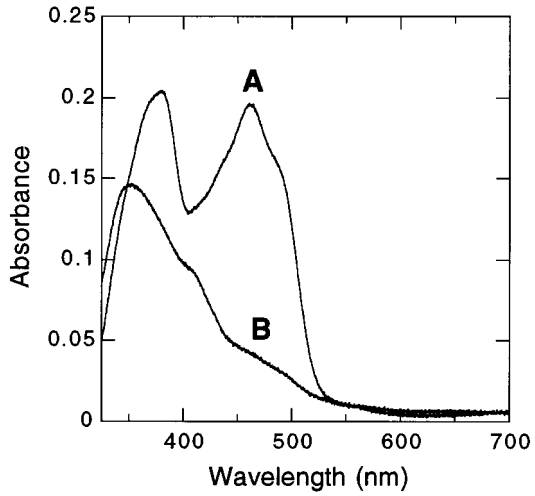

FIGURE 1: Absorbance spectrum of MDH in the oxidized and reduced states. (A) Oxidized MDH, 0.85 mg/mL, in 20 mM potassium phosphate, pH 7.5, with 10% ethylene glycol and 0.1% Triton X-100; (B) after 5 mM (*S*)-mandelate was added.

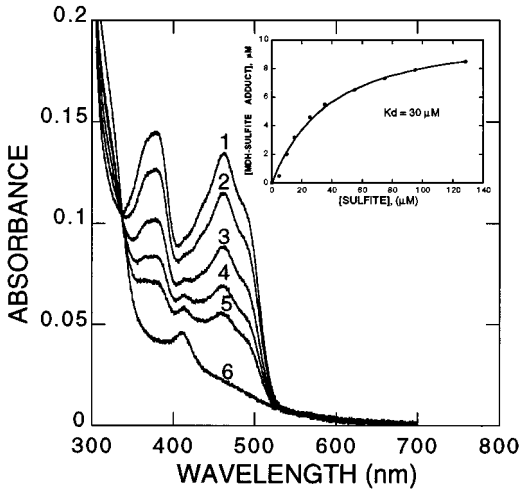

FIGURE 2: Formation of a FMN−sulfite adduct in MDH. MDH (11 μM) was incubated with (1) 0 μM, (2) 10 μM, (3) 25 μM, (4) 55 μM, (5) 95 μM, and (6) 10 mM sodium sulfite in 20 mM potassium phosphate, containing 0.05% Triton X-100 and 5% ethylene glycol at 4 °C. The inset shows a plot of the FMN−sulfite adduct formed versus the total sulfite added. The solid line is a fit to eq 2.

to the expected FMN peaks, and was most likely a membrane-bound cytochrome. We ascertained that this additional peak was not due to an intrinsic cofactor of MDH since the impurity could be partially removed by repeated anion-exchange or gel-filtration chromatography, resulting in increased activity of MDH. However, MDH suffers inactivation due to irreversible loss of FMN on prolonged exposure to buffers of moderate to high ionic strength. This latter observation has also been made for the homologous enzyme, glycolate oxidase (*12*), and may reflect a weaker binding of the cofactor by these proteins. We therefore modified our purification protocol to generate highly pure protein with a minimum number of chromatographic steps. A hexahistidyl tag was engineered at the carboxy terminus of the protein. Following solubilization from the membranes with detergents, the histidine-tagged protein could be purified to homogeneity in a single step on a Ni−NTA affinity column. We confirmed that the histidyl-tagged protein was identical to the native protein in its spectroscopic as well as kinetic properties including substrate isotope effect. Therefore, we did not remove the histidyl tag from the enzyme preparations used in this study.

Figure 1 shows the absorption spectrum of purified MDH with absorbance maxima at 378 and 461 nm. On addition of the substrate, (*S*)-mandelate, the reduced spectrum shows an absorbance maximum at 350 nm. These spectra have not been corrected for light scattering due to detergent micelles, and hence the 378 nm peak appears slightly higher than the 460 nm peak in the oxidized spectrum and the 350 nm peak appears slightly higher than normal for the reduced spectrum. Since MDH does not utilize oxygen as an electron acceptor at an appreciable rate, the reduced spectrum could be obtained under aerobic conditions.

The extinction coefficient of MDH was determined to be 10 400 M^{-1} cm^{-1} at 460 nm, at pH 7.5 and 20 °C in 20 mM potassium phosphate, 10% ethylene glycol, and 0.1% Triton X-100 or 1% Tween 80.

Determination of the pK_a of MDH-Bound FMN. A pH titration of the enzyme-bound FMN at 4 °C revealed that the pK_a is close to that of free FMN in solution, 10.3 (data not shown). Therefore MDH does not lower the pK_a of FMN, in contrast to observations made with some of the oxidases in this family (*12*, *13*).

Formation of a Reversible Adduct with Sulfite. Like the homologous proteins in this flavoenzyme family, MDH forms a reversible adduct of FMN with sulfite, resulting in the disappearance of the 460 nm absorbance peak. A dissociation constant for this adduct could be determined by direct titration of MDH with varying sulfite concentrations (Figure 2). A K_d of 30 μM at 4 °C and pH 7.5 was obtained, which is not affected by different buffer compositions within experimental error. This K_d was well within the range observed for flavoprotein oxidases (*3*, *4*). However, the FMN−sulfite adduct in MDH is not as strong as for other members of this family, notably glycolate oxidase with a K_d of 0.27 μM at 4 °C, the long-chain 2-hydroxy acid oxidase isozymes with K_ds of 2−5 μM at 25 °C, and lactate monooxygenase with a K_d of 0.06 μM at 25 °C (*12*−*14*).

Steady-State Kinetics and Isotope Effects. Steady-state kinetic parameters were obtained in 100 mM potassium phosphate buffer at pH 7.5 by varying both (*S*)-mandelate and DCPIP concentrations. In these assays, BSA and PMS were omitted from the medium since we wanted to test DCPIP and not PMS as the second substrate in our assays. The data fit to a parallel line pattern in double-reciprocal plots (not shown). This implies that when the dye DCPIP is used as the second substrate in our assays, the enzyme follows ping-pong kinetics. The identity of the physiological electron acceptor is not yet known, and hence, it could not be tested as the true second substrate. When 1 mM PMS and 1 mg/mL BSA were included in the assay, the K_m for DCPIP decreased to <10 μM. Ferricyanide also proved to be an effective electron acceptor. However, in this case, it is not possible to include PMS in the assay. Ferricyanide has a much higher K_m (∼9 mM) in the absence of PMS. Therefore, most of our kinetic parameters were obtained by varying the hydroxy acid substrate at a fixed saturating DCPIP concentration (100−150 μM) in the presence of PMS and BSA.

Table 1: Steady-State Kinetic Parameters for MDH with (*S*)- and (*R,S*)-Mandelates[a]

	k_{cat} (s^{-1})	K_m (μM)	KIE
[α-^{1}H]-(*S*)-mandelate/H_2O	290 ± 12	160 ± 10	
[α-^{2}H]-(*S*)-mandelate/H_2O	118 ± 10	167 ± 9	2.5 (substrate)
[α-^{1}H]-(*S*)-mandelate/D_2O	240 ± 18	110 ± 9	1.2 (solvent)
[α-^{1}H]-(*R,S*)-mandelate/H_2O	260 ± 14	330 ± 20	
[α-^{2H}]-(*R,S*)-mandelate/H_2O	105 ± 7	nd	2.5 (substrate)

[a] Assays were carried out in 100 mM potassium phosphate buffer, pH 7.5 at 20 °C, with 100 μM DCPIP, 1 mM PMS, and 1 mg/mL BSA in either H_2O or D_2O. Values of k_{cat} are expressed in terms of moles of substrate reduced per second per mol of enzyme. KIE = substrate and solvent isotope effects on k_{cat}. nd, not determined.

Table 1 summarizes the steady-state kinetic parameters obtained at pH 7.5 with (*S*)- and (*R,S*)-mandelates. Also included are the substrate and solvent kinetic isotope effects at pH 7.5. The substrate kinetic isotope effect (KIE) of 2.5 indicates that the α-carbon−hydrogen bond-breaking step contributes partially to the overall rate of the reaction. However, the KIE is much smaller than the KIEs observed for the homologous enzymes, implying that there may be at least one other step that contributes to the overall rate in MDH. There was no significant solvent isotope effect on k_{cat} for (*S*)-mandelate (values obtained were ∼1.2).

Steady-state kinetic data obtained with a variety of saturated and unsaturated 2-hydroxy acid substrates are shown in Table 2. These data reveal a number of properties of MDH with respect to substrate binding and catalytic preferences. MDH is an efficient enzyme toward its physiological substrate, (*S*)-mandelate, with a specificity constant of $(1-2) \times 10^6$ M^{-1} s^{-1}. This is also true for ring-substituted mandelates (K. S. Rao and B. Mitra, unpublished observations). However, 3-phenyllactate, which differs from (*S*)-mandelate by having an extra methylene bridge between the aromatic phenyl ring and the α-carbon, is a poor substrate with a 500-fold lower k_{cat} and a ∼3000-fold lower k_{cat}/K_m. The same pattern is observed for the pair of substrates (*R,S*)-indoleglycolate and (*R,S*)-3-indolelactate, which differ by an extra methylene bridge between the aromatic indole ring and the α-carbon. Indoleglycolate is comparable to mandelate in terms of catalytic efficiency (∼40% that of mandelate), but 3-indolelactate has a 700-fold lower k_{cat}/K_m. The α-protons of mandelate and indoleglycolate are expected to have pK_as lower than those of 3-phenyllactate and 3-indolelactate by ∼2−3 units. Thus, there is a correlation between higher turnover rates and lower pK_as of the substrate α-proton.

As expected from the above correlation, saturated aliphatic hydroxy acids are poor substrates for MDH with turnover rates that are typically 500−5000-fold lower than that with mandelate (Table 2). Comparison of the K_m data for the 4−8-carbon substrates also indicates that MDH has a large active-site pocket and preferentially binds substrates with longer side chains. Thus, 2-hydroxyoctanoate has a K_m of 0.75 mM compared to a K_m of 32 mM for 2-hydroxybutyrate. The kinetic data also shows that branched-chain hydroxy acids have a somewhat higher affinity than their straight-chain analogues but are slightly less active. We were unable to reliably measure k_{cat} and K_m values for lactate and glycolate because of their very high K_ms.

We also examined three aliphatic 4-carbon substrates with varying degrees of β-unsaturation: 2-hydroxybutyric, 2-hydroxy-3-butenic (vinylglycolic), and 2-hydroxy-3-butynoic acids. The latter is a substrate as well as an irreversible inhibitor of MDH. All three molecules are small hydroxy acids and, not surprisingly, have very low binding affinities for MDH (K_m ∼30 mM). However, in this series, we observe an increase in k_{cat} as the degree of β-unsaturation increases and, correspondingly, the pK_a of the α-proton decreases. 2-Hydroxybutyrate has the lowest turnover rate, 2500-fold lower than with mandelate, whereas 2-hydroxy-3-butynoate has a 67-fold lower rate than mandelate. In fact, 2-hydroxy-3-butynoate has the largest k_{cat} after mandelate and indoleglycolate of the substrates tested in Table 2.

Substrate kinetic isotope effects (KIE) at pH 7.5 are listed in Table 2 for some of the substrates. The KIEs are small for mandelate and indoleglycolate, suggesting that the rate of C−H bond cleavage is only partially rate-limiting for these two substrates. However, 3-phenyllactate and 2-hydroxyoctanoate, slow substrates with no β-unsaturation, have KIEs of 5−6, implying that for these substrates the C−H bond breaking is fully rate-limiting. Vinylglycolate has a KIE of ∼4, which appears to be intermediate between those for (*S*)-mandelate and β-saturated substrates.

2-Hydroxy-3-butynoate as an Irreversible Inhibitor. The acetylenic α-hydroxy acid 2-hydroxy-3-butynoate has been shown to be a substrate as well as a mechanism-based inhibitor for many of the enzymes in the hydroxy acid oxidase family. The inactivation occurs through the formation of a covalent adduct with the FMN. MDH was also observed to be inactivated by this substrate with a rate of inactivation, k_i, of 0.0032 s^{-1} (Figure 3). The K_i for this inhibitor was determined to be 36 mM, in reasonable agreement with the observed K_m of 22 mM. Comparison of the k_i for this inhibitor with its turnover rate gives a ratio of 700 turnovers/inactivation event. When a direct measurement of the ratio of turnover to inactivation was made with an excess of 2-hydroxy-3-butynoate and DCPIP, a value of 755 was obtained. These values are within the range obtained for related enzymes: 3200 for flavocytochrome b_2, 110 for lactate monooxygenase, ≥6 for glycolate oxidase (*15*−*17*). When the inactivation experiments were carried out in the absence of DCPIP but in air-saturated buffer, the rate of inactivation was almost undetectable. This observation is consistent with the fact that 2-hydroxy-3-butynoate is a suicide substrate: inactivation is a consequence of turnover. MDH is a dehydrogenase—it does not utilize oxygen as an electron acceptor efficiently; in the absence of DCPIP and in air-saturated buffer, there is no detectable turnover rate or inactivation with 2-hydroxy-3-butynoate.

pH Dependence of Kinetic Parameters with (S)-Mandelate and (R,S)-3-Phenyllactate. Table 2 shows substrate kinetic isotope effects for (*S*)-mandelate and a few of the tested substrates at pH 7.5. Since the isotope effects at pH 7.5 were smaller for (*S*)-mandelate than for substrates with very low catalytic rates, we decided to investigate whether this was true at all pHs. We therefore undertook a detailed analysis of the pH dependence of the kinetic parameters for MDH for (*S*)-mandelate and a very slow substrate, 3-phenyllactate.

pH Profiles of k_{cat} and k_{cat}/K_m. The pH dependencies of k_{cat} and k_{cat}/K_m for (*S*)-mandelate are shown in Figure 4. Both sets of data fit well to eq 6, which describes a bell-shaped curve with ascending and descending limbs at low and high pHs, respectively. For k_{cat}, a group with pK_a of 5.1 has to be

Table 2: Relative Steady-State Kinetic Parameters at pH 7.5 for MDH with Alternate Substrates[a]

	rel k_{cat}	K_M (mM)	rel k_{cat}/K_M	KIE (k_{cat})
(*R*,*S*)-mandelate	1	0.33 ± 0.02	1	2.5
(*R*,*S*)-indoleglycolate	0.470	0.40 ± 0.03	0.39	3.1
(*R*,*S*)-3-phenyllactate	2×10^{-3}	2.0 ± 0.1	3.3×10^{-4}	5.9
(*R*,*S*)-3-indolelactate	4×10^{-3}	0.9 ± 0.1	1.5×10^{-3}	nd
(*R*,*S*)-2-hydroxyoctanoate	1.9×10^{-3}	0.75 ± 0.1	8.4×10^{-4}	4.8
(*R*,*S*)-2-hydroxyisocaproate	3.1×10^{-3}	4.3 ± 0.2	2.4×10^{-4}	nd
(*R*,*S*)-2-hydroxyhexanoate	1.3×10^{-3}	4.9 ± 0.4	8.8×10^{-5}	nd
(*R*,*S*)-2-hydroxyisovalerate	1.7×10^{-4}	9.5 ± 1.7	5.9×10^{-6}	nd
(*R*,*S*)-2-hydroxyvalerate	1.4×10^{-3}	15.3 ± 1.5	3.0×10^{-5}	nd
(*R*,*S*)-2-hydroxybutyrate	4.0×10^{-4}	32.0 ± 3.5	4.1×10^{-6}	nd
(*R*,*S*)-2-hydroxy-3-butenoate (vinylglycolate)	2.6×10^{-3}	15.4 ± 1.5	2.9×10^{-5}	4.1
(*R*,*S*)-2-hydroxy-3-butynoate	1.5×10^{-2}	22.0 ± 1.5	2.3×10^{-4}	nd

[a] Assay conditions were as in Table 1. k_{cat} and k_{cat}/K_m are relative to (*R*,*S*)-mandelate. nd, not determined.

unprotonated for activity and a second group with pK_a of 9.6 has to be protonated for activity. For the k_{cat}/K_m profile, these two pK_as are slightly shifted inward to 5.5 and 8.9.

The pH dependence of k_{cat} for (*R*,*S*)-3-phenyllactate is shown in Figure 5; the data were fitted to eq 7. In this case, a group with a pK_a of 6.0 has to be unprotonated for activity, and in contrast to (*S*)-mandelate, a group with a pK_a of 8.6 leads to increased activity when it is unprotonated. The data do not display a descending limb at high pH in the pH range tested, 5.5−9.5. Inactivation of enzyme prevented measurements above pH 9.5. Therefore, if there is a group that has to be protonated for activity with (*R*,*S*)-3-phenyllactate, as is the case with (*S*)-mandelate (Figure 4), then it must have a pK_a greater than 10. We also fitted the data to eq 10, which does not take into account the increase in activity or a plateau at intermediate pH. In this case, the fit was significantly worse than to eq 7, though the lower pK_a value did not change.

$$y = \frac{Y_L}{1 + 10^{pK_1 - pH}} \qquad (10)$$

Due to the very low k_{cat} values, and the higher K_m for 3-phenyllactate, the k_{cat}/K_m vs pH values for this substrate had larger errors associated with them, especially at high pH. However, the k_{cat}/K_m vs pH profile was similar to that for (*S*)-mandelate, displaying a bell-shaped dependence on pH (data not shown).

pH Dependence of Primary Substrate Kinetic Isotope Effects. Figure 6 shows the effects of pH on the primary substrate kinetic isotope effects (KIEs) on k_{cat} as well as k_{cat}/K_m for (*S*)-mandelate and the KIE on k_{cat} for (*R*,*S*)-3-phenyllactate. For (*S*)-mandelate, the KIE (k_{cat}) values were ∼2.6 over a wide range of pH, increasing slightly above pH 9. The KIE (k_{cat}/K_m) values were also constant, ∼3.0, at low and neutral pH, increasing at pH values > 9. Since the upper limits of these plots were not well-defined, we did not fit these data to obtain pK_as in the alkaline range. However, we can conclude from Figure 6 that the KIE for MDH with (*S*)-mandelate as substrate ranges from 2.6 to 3.0 at low and intermediate pHs and increases when a group with pK_a of >9 becomes deprotonated. In contrast, (*R*,*S*)-3-phenyllactate displayed a high kinetic isotope effect of >6 that was invariant with pH (the average weighted value was 6.4).

pH Dependence of K_i Values for Competitive Inhibitors. (*S*)-2-Methoxy-2-phenylacetate, (*S*)-1-phenyl-1,2-ethanediol and 2-phenylacetate are all competitive inhibitors of MDH.

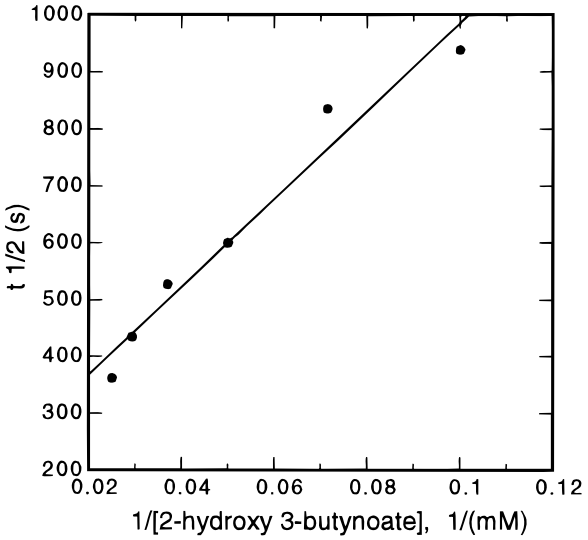

FIGURE 3: Inactivation of MDH by (*R*,*S*)-2-hydroxy-3-butynoate. The half-life of inactivation ($t_{1/2}$) is shown as a function of the reciprocal of inactivator concentration. The enzyme was incubated with various concentrations of (*R*,*S*)-2-hydroxy-3-butynoate in 0.1 M potassium phosphate buffer, pH 7.5 at 20 °C. At fixed time intervals, a 10 μL aliquot was diluted into standard assay buffer and the assay was initiated with the addition of (*S*)-mandelate. $t_{1/2}$ values were determined from plots of remaining activity versus time.

Additionally, (*S*)-3-phenyllactate, a very slow substrate, also acts as a competitive inhibitor. To obtain some idea of the identities of the two active-site residues in MDH that are implicated in the pH−rate profiles, we measured the effects of pH on the inhibition constants of these inhibitors. The results are shown in Figure 7 and summarized in Table 3. 2-Phenylacetate, (*S*)-2-methoxy-2-phenylacetate, and (*S*)-3-phenyllactate all displayed K_i values that fit well to eq 8. Binding affinity increased at low pH with pK_a values of 5.0−6.5 and decreased at high pH with pK_a values of 9.4−9.5. The limiting values for the inhibition constants were found to be 3.9, 0.8, and 0.7 mM, respectively, for 2-phenylacetate, (*S*)-2-methoxy-2-phenylacetate, and (*S*)-3-phenyllactate at acidic pH and 12.1, 13.5, and 8.1 mM at neutral pH. The fits shown in Figure 7 assume that the carboxylic acids, that is, the protonated forms of these three inhibitors bind as tightly to the enzyme as the unprotonated, carboxylate anionic forms. The pK_as of the carboxylate groups of the inhibitors and substrates are 4.3 for 2-phenylacetate, 3.1 for (*S*)-2-methoxy-2-phenylacetate, 3.7 for (*S*)-3-phenyllactate, and 3.1−3.4 for (*S*)-mandelate (ACD Labs). When the pH

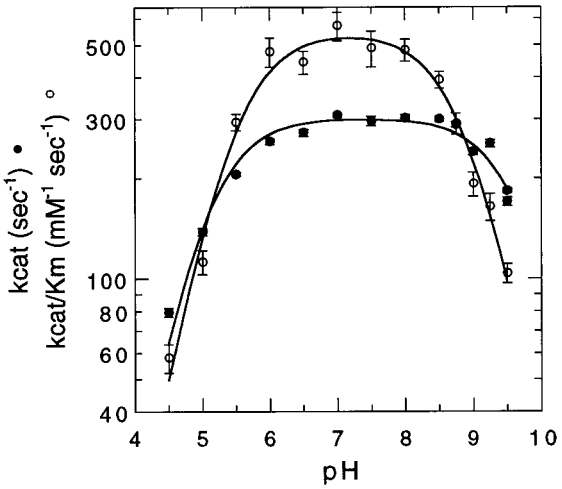

FIGURE 4: pH dependence of k_{cat} (●) and k_{cat}/K_m (○) values for MDH at 20 °C with (*S*)-mandelate. The lines are fits to eq 6. The buffer used over the entire pH range was made up of 0.025 M boric acid, 0.025 M potassium phosphate, 0.025 M Tris, and 0.025 M succinic acid. At each pH, the final ionic strength was maintained at 0.18 with the addition of KCl. Assays were performed by measuring the decrease in absorbance of DCPIP at 522 nm in the presence of 1 mg/mL BSA and 1 mM PMS.

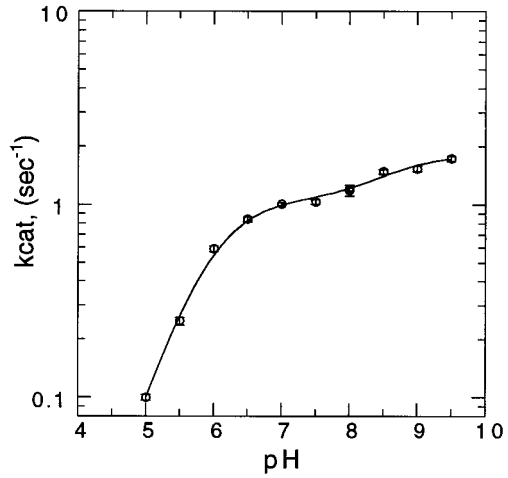

FIGURE 5: pH dependence of k_{cat} values for MDH at 20 °C with (*R*,*S*)-3-phenyllactate. The solid line is a fit to eq 7. The assay buffer was the same as in Figure 4, except that PMS was omitted.

dependence of the inhibition constants were refitted to eq 8 using these pK_as and assuming that only the carboxylate anionic forms of the inhibitors bind to the enzyme, the pK_a values did not change in any significant way. The fourth competitive inhibitor we tested, (*S*)-1-phenyl-1,2-ethanediol, lacks a carboxylate functionality. The pH dependence of this inhibitor is best fitted to the simple eq 9, which indicates that the binding affinity decreases sharply at low pH with a pK_a of 5.4 but does not change at high pH. Taken together, these studies with the four competitive inhibitors suggest that MDH has two active-site residues with apparent pK_as of ~5.4 and ~9.4, which are important in binding. It is clear that the residue with the apparent pK_a of 9.4 binds the anionic carboxylate group of substrates/inhibitors.

DISCUSSION

In this study, we report the first mechanistic characterization of MDH, one of the newest members of the FMN-dependent α-hydroxy acid oxidase/dehydrogenase family.

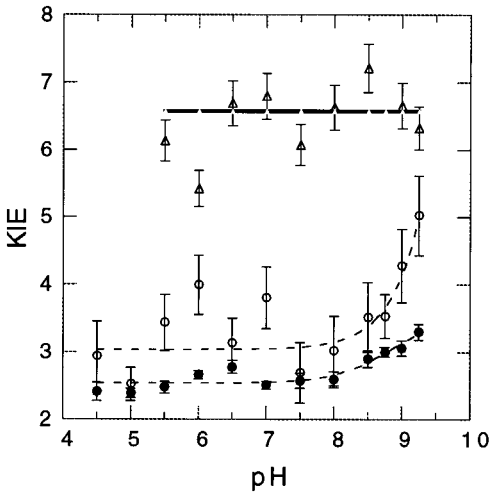

FIGURE 6: pH dependence of substrate kinetic isotope effect (KIE) values for MDH: (●), KIE(k_{cat}) for (*S*)-mandelate; (○) KIE(k_{cat}/K_m) for (*S*)-mandelate; (△) KIE(k_{cat}) for (*R*,*S*)-3-phenyllactate at 20 °C. The solid line is drawn through the weighted mean of the KIE data for (*R*,*S*)-3-phenyllactate. The dashed lines are smooth lines through the points.

MDH differs from the more well-characterized members of this family in being a membrane-bound protein that does not utilize oxygen as its ultimate oxidant but an external electron acceptor that is most likely a member of the membrane electron transport chain. Also, in contrast to the homologous enzymes, MDH uses a large, aromatic substrate. These differences make MDH an attractive enzyme for exploring mechanistic questions such as the basis of unreactivity toward oxygen, the origin of substrate specificities, and correlation of the pK_a of the substrate α-proton with reaction rates, among others.

The cloning, overexpression, and purification protocol for this enzyme has been previously described (*9*). In this work, we added a hexahistidyl tag at the carboxyl terminus of MDH to facilitate its purification in one step. The hexahistidyl-tagged protein has identical properties to the native protein. In common with the other α-hydroxy acid oxidases and dehydrogenases, MDH has a noncovalently bound FMN that is reduced by the substrate, (*S*)-mandelate. However, in contrast to the oxidases, the MDH-bound reduced FMN does not react with oxygen at a catalytically significant rate. A pH titration of the MDH-bound FMN revealed that MDH does not lower the pK_a of enzyme-bound FMN. This result is in contrast to glycolate oxidase and hydroxy acid oxidase, where the enzymes perturb the pK_a of FMN to 6.4 and 7.5−7.9, respectively (*12*, *13*). It is to be noted that the Y129F mutant of glycolate oxidase does not significantly lower the pK_a of FMN (*18*).

In common with other flavin-dependent α-amino- or α-hydroxy acid oxidases and dehydrogenases, MDH forms a reversible covalent FMN−sulfite adduct. In MDH, the adduct has a K_d of 30 μM at 4 °C, which is 10−500-fold greater than the K_d values reported for the other enzymes of the 2-hydroxy acid oxidase family. The strength of the FMN−sulfite adduct may depend on the electrophilicity of FMN in the oxidized enzyme, as well as interactions of the adduct with active-site residues. Tegoni and Mathews (*19*) have shown that the sulfite oxygens of the FMN−sulfite adduct in the crystal structure of flavocytochrome b_2 interact

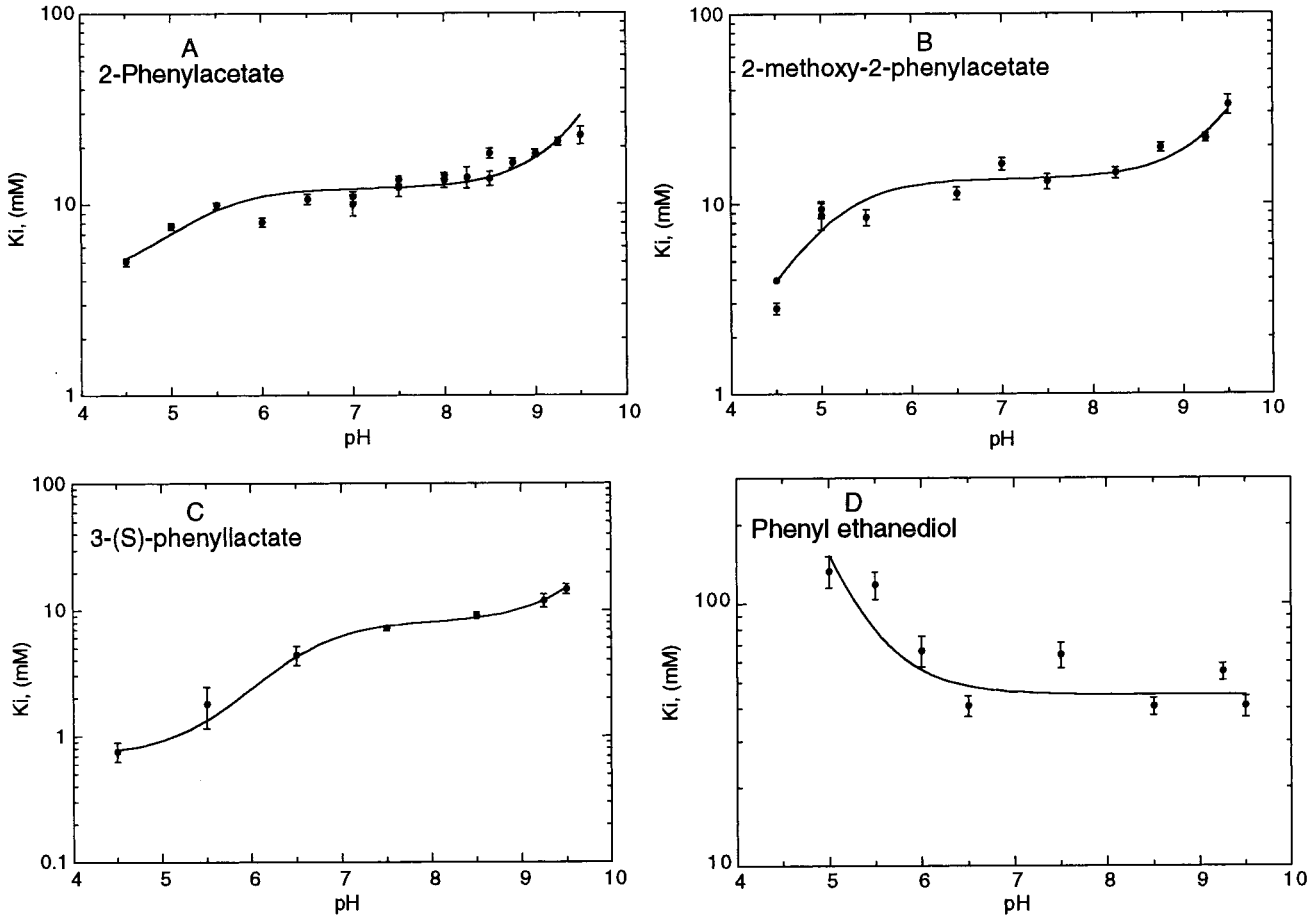

FIGURE 7: pH dependence of inhibition constants for the competitive inhibitors of MDH: (A) 2-phenylacetate, (B) (*S*)-2-methoxy-2-phenylacetate, (C) (*S*)-3-phenyllactate, and (D) (*S*)-1-phenyl-1,2-ethanediol. The lines are fits to eqs 8 (A−C) and 9 (D).

Table 3: pK_a Values for Mandelate Dehydrogenase for Steady-State Kinetic Parameters[a]

	pK_1	pK_2	pK_3	limiting values	eq
k_{cat} (SM)	5.1 ± 0.1	9.6 ± 0.1		301 ± 2 s^{-1}	6
k_{cat}/K_M (SM)	5.5 ± 0.1	8.9 ± 0.1		545 ± 23 s^{-1}·mM^{-1}	6
k_{cat} (PL)	6.0 ± 0.1		8.6 ± 0.1	1.1 ± 0.1 s^{-1} 1.8 ± 0.1 s^{-1}	7
KIE k_{cat} (SM)		> 9		2.6	
KIE k_{cat}/K_m (SM)		> 9		3.0	
K_i (PA)	5.2 ± 0.1	9.4 ± 0.1			8
K_i (MPA)	5.0 ± 0.2	9.4 ± 0.1			8
K_i (SPL)	6.5 ± 0.2	9.5 ± 0.1			8
K_i (PE)	5.4 ± 0.1				9

[a] SM = (*S*)-mandelate; PL = (*R,S*)-3-phenyllactate; PA = phenylacetate; MPA = (*S*)-2-methoxy-2-phenylacetate; SPL = (*S*)-3-phenyllactate; PE = (*S*)-1-phenyl-1,2-ethanediol.

with the conserved tyrosine, histidine, and arginine residues implicated in catalysis. The higher K_d in MDH may imply that the FMN in this enzyme is less electrophilic. However, a more likely explanation is that the larger active site in MDH does not allow strong interactions of the conserved active-site residues with the FMN−sulfite adduct. MDH has to accommodate a bulkier and more constrained substrate than other enzymes in this family and consequently has a larger active-site cavity.

2-Hydroxy-3-butynoate is both a substrate and an inactivator for the hydroxy acid oxidases. It has been proposed that the mechanism of inactivation is due to the generation of a carbanion at the active site, which subsequently forms an irreversible adduct with FMN. MDH is also inactivated by this acetylenic hydroxy acid. The ratio of turnover to inactivation obtained for MDH is ~700 and well within the range observed for other enzymes.

Substrate Specificity. Steady-state kinetics show that MDH follows ping-pong kinetics when the dye DCPIP is used as the second substrate (data not shown). Table 2 summarizes kinetic parameters obtained for MDH at pH 7.5 with α-hydroxy acid substrates with different side-chain sizes as well as very different pK_as of the α-proton. The data indicate that MDH is specific toward large substrates. Small substrates have high K_ms as well as low k_{cat}s; no rate could be detected with lactate or glycolate. These observations suggest that the active site of MDH possesses a large hydrophobic cavity that accommodates the side chains of large substrates. It has

been recently proposed that a few nonconserved residues may control substrate specificity in this enzyme family. For example, tryptophan 108 in glycolate oxidase, alanine 95 in L-lactate oxidase, alanine 198, leucine 230, and isoleucine 326 in flavocytochrome b_2, and alanine 110 in MDH control substrate specificity (*20*−*23*).

Correlation of α-Proton pK_a with k_{cat} and KIE. The catalytic mechanism in this enzyme family has been postulated to proceed via the initial abstraction of the substrate α-proton, leading to the formation of a carbanion intermediate. However, there is some controversy regarding the mechanism of this carbon−hydrogen bond cleavage step, with some workers supporting a simple direct hydride transfer from the substrate to FMN (*5*, *7*). MDH appears to be ideally suited to address this question for the following reasons. Its physiological substrate has an aromatic ring directly attached to the α-carbon atom, leading to a lower pK_a of the α-proton than is the case for glycolate, lactate, and other saturated α-hydroxy acids. If MDH has been optimized to oxidize mandelate, then in the case of a carbanion mechanism, it should not be able to efficiently oxidize substrates that have higher α-proton pK_as. Additionally, the α-carbon−hydrogen bond-breaking step in MDH is partially rate-limiting as shown by the relatively small substrate KIE of 2.5 obtained with (*S*)-mandelate. This indicates that another catalytic step also contributes to the overall reaction rate in MDH, most probably electron-transfer from the carbanion to the flavin for the natural substrate. This is in contrast to the other enzymes in this family that utilize saturated α-hydroxy acids, where the KIEs range from 4 to 6 and the α-carbon−hydrogen bond-breaking step is believed to be fully rate-limiting. Therefore, we set out to obtain evidence in support of either a "carbanion" or a "hydride transfer" mechanism for MDH, using substrates with highly different pK_as of the α-proton. We expected that this pK_a should correlate with the catalytic rate as well as substrate kinetic isotope effect if the mechanism involves a carbanion intermediate. However, it would not greatly influence a reaction proceeding through the transfer of a hydride equivalent.

Preliminary observations suggested to us that very small changes in the pK_a of the α-proton, as are found among different ring-substituted mandelates with electron donating/withdrawing substituents, may not be sufficient to measurably affect the k_{cat} and the KIE. When these substituted mandelates were tested with MDH, they did not result in significantly different KIEs or k_{cat}s (Rao and Mitra, unpublished observations). Such structure−activity studies with the flavocytochrome b_2 (mandelate dehydrogenase) from *Rhodotorula graminis* (*24*) and with a mutant of lactate oxidase (*6*) have been reported. No correlation could be established between the effect of the ring substituent and the nature (electron-rich or -deficient) of the reaction intermediate. Therefore, for this study, we chose substrates with very different pK_as of their α-protons. The substrate pair mandelate and 3-phenyllactate, as well as indoleglycolate and 3-indolelactate, differ by an extra methylene group between the aromatic ring and the α-carbon. As a consequence, the pK_as of the α-protons of mandelate and indoleglycolate are smaller by 2−3 units. The α-protons of fully saturated aliphatic hydroxy acids also have pK_as that are 3 units or more greater than that of mandelate. The data in Table 2 clearly demonstrates that 300−6000-fold higher k_{cat}s are obtained with mandelate and indoleglycolate compared to 3-phenyllactate, 3-indolelactate, and saturated aliphatic hydroxy acids. Also, the KIE increases from 2.5−3 to 5−6 for these slow substrates, indicating that for the latter, the carbon−hydrogen bond-breaking step is fully rate-limiting. This difference in KIE for fast and slow substrates is maintained across the entire optimal pH range, as shown in our pH studies. We also tested three small, aliphatic substrates, 2-hydroxybutyric, 2-hydroxy-3-butenoic (vinylglycolic), and 2-hydroxy-3-butynoic acids with varying degrees of β-unsaturation. These hydroxy acids have very high K_ms, ranging from 15 to 30 mM. However, we observed that the k_{cat} was 38-fold greater for 2-hydroxy-3-butynoic acid and 6-fold greater for vinylglycolic acid compared to 2-hydroxybutyric acid, one of the slowest substrates we tested. Thus, once again, β-unsaturated substrates, which are expected to have lower α-proton pK_as, have higher k_{cat}s.

Scheme 1

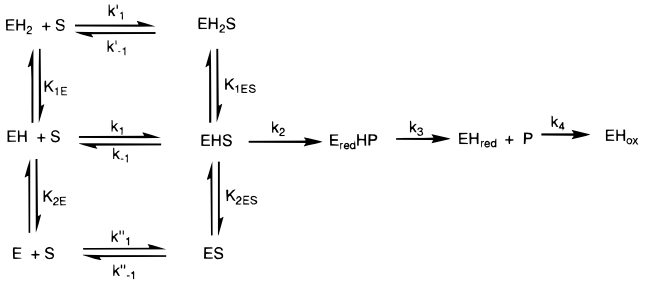

Therefore, our alternate substrate studies suggest that the β-unsaturation afforded by the α-phenyl, α-indolyl, α-vinyl, or α-acetylenic groups, which lowers the pK_a of the α-proton, leads to a faster catalytic rate and a lower isotope effect in MDH. When the pK_a of the α-proton is higher than that of mandelate by 3 units or more, the C−H bond-breaking step becomes fully rate-limiting and the overall rate decreases by 300-fold or more. This correlation between the pK_a of the substrate α-proton, k_{cat}, and KIE support a mechanism with a carbanion intermediate. A mechanism in which the C−H bond breaks with the generation of a hydride ion is difficult to reconcile with our data.

pH studies of (S)-Mandelate and (R,S)-3-Phenyllactate. We carried out a detailed pH analysis of the kinetic parameters for MDH for two reasons. First, we hoped to identify the mechanistic role of pH-dependent catalytic residues in MDH. Second, we wanted to confirm that the isotope effects for (*S*)-mandelate and other slow substrates that we determined at pH 7.5 were, in fact, representative values over the optimal pH range. We determined the pH dependence of k_{cat} and k_{cat}/K_m for (*S*)-mandelate and a typical slow substrate, (*R*,*S*)-3-phenyllactate. With (*S*)-mandelate, the k_{cat}/K_m pH profile indicates that a group with a pK_a of 5.5 has to be unprotonated and a group with a pK_a of 8.9 has to be protonated for activity (Scheme 1). The k_{cat} pH profile is very similar, except that the two pK_as are shifted outward to 5.1 and 9.6. It is likely that the acidic and basic groups revealed in the k_{cat}/K_m and k_{cat} pH profiles correspond to the same residues. Typically, the k_{cat}/K_m pH profile represents pK_as of residues in the free enzyme or free substrate and the k_{cat} pH profile represents pK_as in the enzyme−substrate complex (*25*). The pK_a values from the k_{cat}/K_m pH profile (Figure 4) most likely represent residues in free MDH, since the free substrate does not have an ionizable group in the

pH range tested [pK_a of the carboxylic acid proton of (*S*)-mandelate is 3.1−3.4] and (*S*)-mandelate does not appear to be a sticky substrate. For a sticky substrate, $k_2 \gg k_{-1}$ (Scheme 1) (*25*). The pK_a values obtained from the k_{cat}/K_m pH profile for a sticky substrate should be shifted *outward* compared to those of the k_{cat} pH profile (*25*). Also, in the case of a sticky substrate, the substrate KIE decreases at the pH optimum, as opposed to what we observe for (*S*)-mandelate, where no acidic pK_a is observed in the KIE pH profile (Figure 6). Thus, it is likely that two residues with apparent pK_as of 5.5 and 8.9 in the free enzyme have their pK_as shifted to 5.1 and 9.6 in the enzyme−substrate complex. Identical pH profiles for k_{cat} and k_{cat}/K_m have previously been observed for another enzyme in this family, flavocytochrome b_2 from *S. cerevisiae*, with lactate (*26*).

The k_{cat}/K_m pH profile for (*R*,*S*)-3-phenyllactate was similar to that for (*S*)-mandelate. However, the k_{cat} pH profile for this slow substrate was somewhat different. In the acidic pH range, a pK_a of 6.0 was observed, which probably belongs to the same residue seen in the pH profile with (*S*)-mandelate. In contrast to (*S*)-mandelate, there was no decrease in activity at alkaline pH up to the highest pH tested, 9.5. It is possible that (*R*,*S*)-3-phenyllactate perturbs the alkaline pK_a of 8.9 in the free enzyme to a value that is >10 in the enzyme−substrate complex. An intermediate pK_a was observed for (*R*,*S*)-3-phenyllactate, which is not apparent for (*S*)-mandelate. In this case, the deprotonation of a group with a pK_a of 8.6 increases the rate by ∼75%. When we fitted the data for (*S*)-mandelate to three pK_as including this intermediate pK_a, we obtained a fit that showed a small increase in activity at intermediate pH but was not significantly better.

The KIE pH profile on k_{cat} for (*S*)-mandelate is constant in the acidic and neutral pH range (2.6), increasing at high pH with a pK_a > 9. The KIE on the k_{cat}/K_m also displays essentially the same pH profile, with a KIE of 3.0 increasing at high pH with a pK_a > 9. This increase in the KIE at high pH appears to be due to an incorrectly protonated and therefore less active form of the enzyme. This conclusion is supported by the observation that the k_{cat}/K_m decreases at high pH. The KIE pH profile of (*R*,*S*)-3-phenyllactate shows a KIE of ∼6.4 that is invariant with pH.

Identity of the Residue with an Apparent pK_a of 5.5. The pH dependence of the kinetic parameters and the KIEs in MDH suggests that a group with an apparent pK_a of 5.5 in the free enzyme is critical for activity; it is involved in the isotope-sensitive step of the mechanism (*27*) (Scheme 1). The active sites of the FMN-dependent α-hydroxy acid oxidases and dehydrogenases have a conserved histidine, which has been proposed to act as the base that abstracts the α-proton leading to the formation of the carbanion (*28*). On the basis of previous homology and modeling studies of MDH, we conclude that this residue is histidine 274 (*9*). This histidine is essential for activity, since the H274N mutant is completely inactive (*29*). Similar results were obtained for flavocytochrome b_2 and lactate monooxygenase (*30*, *31*). It seems likely that the apparent pK_a of 5.5 belongs to histidine 274. Protonation results in an increase in [EH_2] and a decrease in k_{cat}. We have recently obtained further evidence that this pK_a assignment is correct through characterization of the pH dependence of the chemically rescued activity of site-specific mutations of histidine 274 (Lehoux and Mitra, manuscript submitted).

Identity of the Residue with an Apparent pK_a of 8.9. To identify the residue with a pK_a of 8.9, we characterized the pH dependence of K_i values of four competitive inhibitors of MDH. Three inhibitors with carboxylate groups, (*S*)-3-phenyllactate, (*S*)-2-methoxy-2-phenylacetate, and 2-phenylacetate, were used, as well as one lacking a carboxylate group, (*S*)-1-phenyl-1,2-ethanediol. The inhibitors with carboxylate groups all showed the same pH profile. The binding affinity is highest at very low pH, decreasing as the pH is raised with a pK_a of 5.0−6.5, and further decreasing at alkaline pH with a pK_a of ∼9.4. (*S*)-1-Phenyl-1,2-ethanediol displayed a very different pH profile. The binding affinity decreased at low pH with a pK_a of 5.4 and did not change at high pH. Comparing these pK_a values to those obtained with the k_{cat} and k_{cat}/K_m pH profiles, it seems likely that the same two groups are involved in binding these competitive inhibitors as well. It is apparent that the inhibitors with a carboxylate group do not bind tightly when the residue with an apparent pK_a of 9.4 is deprotonated, whereas the binding of an uncharged inhibitor is unaffected by the protonation state of this residue. From the three-dimensional structures of flavocytochrome b_2 and glycolate oxidase, it is clear that this residue must be one of the two conserved arginines that coordinate with the substrate carboxylate group—arginine 165 or arginine 277 in MDH as revealed by homology studies (*32*−*34*, *9*). The unusually low pK_a of 8.9 for an arginine residue in the free enzyme is most likely due to the close proximity of the two arginines. The second arginine of this pair would be expected to have a pK_a that is close to normal. In flavocytochrome b_2, the residue homologous to arginine 277 interacts directly with the carboxylate group of the product, pyruvate (*32*). However, a three-dimensional structure of glycolate oxidase obtained with an inhibitor bound shows that both arginines participate in the binding of the carboxylate group of the inhibitor (*33*). We cannot be certain which arginine, 165 or 277, has the apparent pK_a of 8.9. We have observed that the R277M mutant of MDH is completely inactive, whereas the R277K mutant has a ∼50-fold higher K_m, a ∼80-fold lower k_{cat}, and a kinetic isotope effect of ∼4.6 (*29*). These results suggest that arginine 277 may be important for binding and intermediate stabilization and we therefore tentatively assign the pK_a of 8.9 to this residue. However, this conclusion has to be verified in future studies.

When the k_{cat}/K_m pH profile reflects ionizations in the free enzyme, the pK_as obtained should be similar to those obtained in the inhibitor K_i profiles. However, in our case, the apparent pK_a of 8.9 for arginine 277 obtained in the k_{cat}/K_m profile is slightly lower than the pK_a of 9.4 obtained in the K_i profiles. A possible explanation for this discrepancy may be that at alkaline pH there are actually two pK_as for the inhibitor pH profile, one reflecting the free enzyme, and the other the enzyme−inhibitor complex. This is the case when both the protonated and unprotonated states of the enzyme can bind the inhibitor, but the latter with lower affinity (*35*). The pK_a due to the enzyme−inhibitor complex is displaced to a higher pK_a value relative to the free enzyme. The measured pK_a is then an average of these two pK_as. The lack of data beyond pH 9.5 precludes our assignment of a correct pK_a for the enzyme−inhibitor complex; however, an inspection of Figure 7 does support a pK_a of ∼9.0 for the free enzyme, as was also obtained from the k_{cat}/K_m pH profile.

Scheme 2

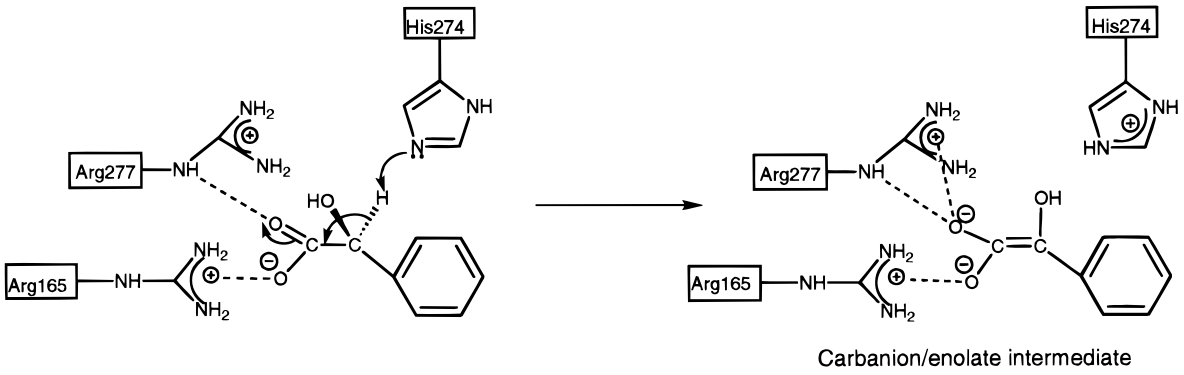

At low pH, all the competitive inhibitors display a pK_a of 5.0−5.4, with the exception of (*S*)-3-phenyllactate, which has a pK_a of 6.5. It is likely that these pK_as belong to the same residue; the reason for the higher pK_a obtained for (*S*)-3-phenyllactate is not clear. The pK_a value of 5.0−5.4 agrees well with the pK_a of 5.5 seen in the k_{cat}/K_m pH profile. As noted above, we believe that this pK_a belongs to histidine 274, which is the base that is proposed to abstract the α-proton. For (*S*)-1-phenyl-1,2-ethanediol, the binding affinity decreases when this residue is protonated. An identical behavior is observed for the K_m pH profile for (*S*)-mandelate (data not shown). Steric interference may exist between the α-proton of the substrate/inhibitor and the protonated N-ϵ of the histidine residue leading to weaker binding. The active site of flavocytochrome b_2 has been modeled with the substrate lactate (*28*). In this model, the substrate is held in a productive conformation through ionic interactions of the carboxylate group with an arginine residue and hydrogen-bonding of the hydroxyl group with a conserved tyrosine residue. The α-proton points toward the N-ϵ of the histidine residue—an optimal geometry for proton abstraction. It is likely that when the α-hydroxyl group of an (*S*)-enantiomer of a substrate/inhibitor molecule interacts with the conserved active-site tyrosine residue, the α-proton and the histidine N-ϵ are juxtaposed.

For the inhibitors with carboxylate groups, the binding affinity *increases* when the histidine is protonated. A simple explanation is that there is a favorable electrostatic interaction between the protonated histidine and the carboxylate groups that leads to stronger binding. This electrostatic interaction would more than compensate for any steric interference.

Catalytic Functions of Histidine 274 and Arginine 277. The pH studies presented in this paper show that histidine 274 has to be unprotonated for activity. The substrate kinetic isotope effect remains unchanged when this residue is unprotonated. These observations are in agreement with the proposal that it is the base that abstracts the substrate α-proton, leading to the formation of a carbanion. Arginine 277 (or arginine 165) is a residue that is critical for substrate binding. Our pH studies indicate that it is also important for activity in its protonated form. When this residue is unprotonated, the activity decreases and the KIE increases. The isotope effect results imply that it stabilizes an intermediate that is concomitant with the α-carbon−hydrogen bond-breaking step. This observation fits in nicely with a carbanion mechanism, where the protonated arginine is critical for stabilizing the carbanion/enolate intermediate. However, it is difficult to imagine why the isotope effect would increase in a "hydride transfer" mechanism, or indeed, why the activity would decrease, when this arginine is deprotonated. On the basis of our pH and isotope effect studies, we propose that histidine 274 and most likely arginine 277 generate and stabilize a carbanion/enolate intermediate in the first step of the reaction catalyzed by MDH (Scheme 2).

Conclusion. In this work, we report the first characterization of MDH, one of the newer members of the FMN-dependent α-hydroxy acid oxidase/dehydrogenase family. We show that MDH is a representative member of the family of FMN-dependent α-hydroxy acid oxidases/dehydrogenases. Using substrates with different side-chain sizes, we have shown that MDH has a large substrate binding pocket at the active site. We observed a good correlation between the pK_a of the substrate α-proton and the catalytic rate as well as the substrate kinetic isotope effect. This observation is in perfect agreement with a "carbanion" mechanism but is difficult to explain in the context of a "hydride transfer" mechanism. Finally, we carried out detailed pH studies of MDH, including isotope effects and competitive inhibitors, the first comprehensive study of its kind in this enzyme family. Our results show that unprotonated histidine 274 and a protonated arginine are important for catalysis; this arginine is also important for substrate binding. It has an unusually low pK_a of 8.9. We propose that this arginine, most likely arginine 277, is critical for stabilizing the enolate intermediate generated during the reaction mechanism.

ACKNOWLEDGMENT

We thank Mr. Song Li for assistance in the early part of this work. We are indebted to Professor Shahriar Mobashery and Mr. Jalal Haddad for help with the synthesis protocol for sodium indole glycolate. Professor John Gerlt is gratefully acknowledged for the gift of plasmids carrying the mandelate racemase genes.

REFERENCES

1. Tsou, A. Y., Ransom, S. C., Gerlt, J. A., Buechter, D. D., Babbitt, P. C., and Kenyon, G. L. (1990) *Biochemistry 29*, 9856−9862.
2. Diep Le, K. H., and Lederer, F. (1991) *J. Biol. Chem. 266*, 20877−20881.
3. Ghisla, S., and Massey, V. (1991) in *Chemistry and Biochemistry of Flavoenzymes* (Müller, F., Ed.), Vol. II, pp 243−289, CRC Press, Boca Raton, FL.
4. Lederer, F. (1991) in *Chemistry and Biochemistry of Flavoenzymes* (Müller, F., Ed.) Vol. II, pp 153−242, CRC Press, Boca Raton, FL.

5. Pollegioni, L., Blodig, W., and Ghisla, S. (1997) *J. Biol. Chem. 272*, 4924−4934.
6. Yorita, K., Janko, K., Aki, K., Ghisla, S., Palfey, B. A., and Massey, V. (1997) *Proc. Natl. Acad. Sci. U.S.A. 94*, 9590−9595.
7. Mattevi, A., Vanoni, M. A., Todone, F., Rizzi, M., Teplyakov, A., Coda, A., Bolognesi, M., and Curti, B. (1996) *Proc. Natl. Acad. Sci. U.S.A. 93*, 7496−7501.
8. Li, R., Powers, V. M., Kozarich, J. W., and Kenyon, G. L., (1995) *J. Org. Chem. 60*, 3347−3351.
9. Mitra, B., Gerlt, J. A., Babbitt, P. C., Woo, C. W., Kenyon, G. L., Joseph, D., and Petsko, G. A. (1993) *Biochemistry 32*, 12959−12967.
10. Schowen, B., and Schowen, R. L. (1982) *Methods Enzymol. 87*, 551−606.
11. Ellis, K. J., and Morrison, J. F. (1982) *Methods Enzymol. 87*, 405−426.
12. Macheroux, P., Massey, V., Thiele, D. J., and Volokita, M. (1991) *Biochemistry 30*, 4612−4619.
13. Belmouden, A., and Lederer, F. (1996) *Eur. J. Biochem. 238*, 790−798.
14. Massey, V., Muller, F., Feldberg, R., Schuman, M., Sullivan, P. A., Howell, L. G., Mayhew, S. G., Matthews, R. G., and Foust, G. P. (1969) *J. Biol. Chem. 244*, 3999−4006.
15. Pompon, D., and Lederer, F. (1985) *Eur. J. Biochem. 148*, 145−154.
16. Ghisla, S., Ogata, H. Massey, V. Schonbrunn A., Abeles, R., and Walsh, C. T. (1976) *Biochemistry 15*, 1791−1797.
17. Fendrich, G., and Ghisla, S. (1982) *Biochim. Biophys. Acta 702*, 242−248.
18. Macheroux, P., Kieweg, V., Massey, V., Soderlind, E., Stenberg, K., and Lindqvist, Y. (1993) *Eur. J. Biochem. 213*, 1047−1054.
19. Tegoni, M., and Mathews, F. S. (1988) *J. Biol. Chem. 263*, 19278−19281.
20. Stenberg, K., Clausen, T., Lindqvist, Y., and Macheroux, P. (1995) *Eur. J. Biochem. 228*, 408−416.
21. Yorita, K., Aki, K., Ohkuma-Soyejima, T., Kokubo, T., Misaki, H., and Massey, V. (1996) *J. Biol. Chem. 271*, 28300−28305.
22. Sinclair, R., Reid, G. A., and Chapman, S. K. (1998) *Biochem J. 333*, 117−120.
23. Lehoux, I., and Mitra, B. (1997) *FASEB J. 11* (9), 889.
24. Smekal, O., Reid., G. A., and Chapman, S. K. (1994) *Biochem. J. 297*, 647−652.
25. Cleland, W. W. (1982) *Methods Enzymol. 87*, 309−405.
26. Suzuki, H., and Ogura, Y. C. (1970) *J. Biochem. (Tokyo) 67*, 291−295.
27. Cook, P. F., and Cleland, W. W. (1981) *Biochemistry 20*, 1797−1805.
28. Reid, G. A., White, S., Black, M. T., Lederer, F., Mathews, F. S., and Chapman, S. K. (1988) *Eur. J. Biochem. 178*, 329−333.
29. Lehoux, I., and Mitra, B. (1996) in *Flavins and Flavoproteins* (Stevenson, K., Massey, V., and Williams, C. H., Eds.) pp 567−570, Walter de Gruyter, Berlin and New York.
30. Gaume, B. Sharp, R. E., Manson, F. D. C., Chapman, S. K., Reid, G. A., and Lederer, F. (1995) *Biochimie 77*, 621−630.
31. Muh, U., Williams, C. H., and Massey, V. (1994) *J. Biol. Chem 269*, 7989−7993.
32. Xia, Z., and Mathews, F. S. (1990) *J. Mol. Biol. 212*, 837−863.
33. Stenberg, K., and Lindqvist, Y. (1997) *Protein Sci. 6*, 1009−1015.
34. Lindqvist, Y., Branden, C.-I., Mathews, F. S. and Lederer, F. (1991) *J. Biol. Chem. 266*, 3198−3207.
35. Cleland, W. W. (1977) *Adv. Enzymol. Relat. Areas Mol. Biol. 45*, 273−387.

BI990024M